

Optimal Extraction with Sub-sampled Line-Spread Functions

Nicholas R. Collins¹

Science Systems and Applications, Incorporated, 5900 Princess Garden Parkway, Suite 300, Lanham, MD 20706

Theodore Gull and Chuck Bowers

NASA's GSFC, Code 681, Greenbelt, MD 20771

Don Lindler¹

Sigma Space Corporation, 9801 Greenbelt Road, Lanham, MD 20706

Abstract. STIS long-slit medium resolution spectra reduced in CALSTIS extended-source mode with narrow extraction heights (GWIDTH = 3 pixels) show photometric uncertainties of $\pm 3\%$ relative to point-source extractions. These uncertainties are introduced through interpolation in the spectral image rectification processing stage, and are correlated with the number of pixel crossings the spectral profile core encounters in the spatial direction.

The line-spread-function may be determined as a function of pixel crossing-position from calibration data sub-sampled in the spatial direction. This line spread function will be applied to science data to perform optimal extractions and point-source de-blending. Wavelength and breathing effects will be studied. Viability of the method to de-convolve extended source "blobs" will be investigated.

1. Introduction

In the course of analyzing rectified long-slit spectral observations of nebular targets such as η -Carinae, or of crowded stellar fields, it may be desirable to use a small spectral extraction height to avoid contamination from neighboring sources. Such extractions suffer from $\pm 3\%$ systematic uncertainties introduced by the interpolation step during the spectral image rectification.

We investigate the viability of an optimal extraction procedure that uses the cross-dispersion profile of the STIS long-slit data to improve the extraction of isolated sources and to de-blend neighboring sources.

This work is in progress. To date, we have used a standard star cross-dispersion profile to perform an optimal extraction of the same and other isolated standard stars. We have tested the viability of de-blending point sources by creating a model data set with two point-source spectra of known intensity and relative position. Work remains to be done on improving the point-source de-blending solution and on extending the algorithm to handle resolved sources. Limitations of the method with respect to deriving a cross-dispersion profile from one observation to perform the optimal extraction of another observation include the MSM-repeatability and the focus changes induced by *HST* "breathing."

¹NASA's GSFC, Code 681, Greenbelt, MD 20771

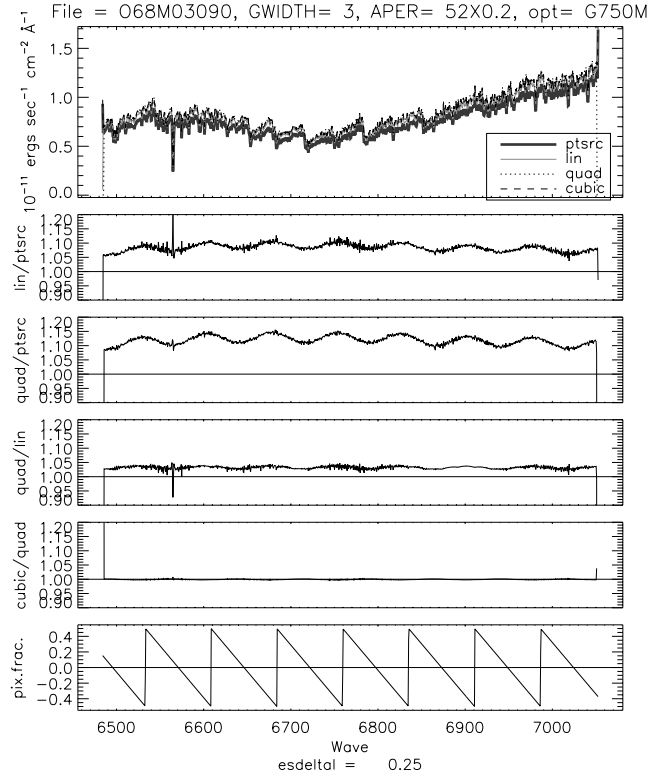


Figure 1. Comparison of extended-source (3-pixel) and point-source (7-pixel) spectral extractions. Top to bottom: All extractions, extended-source (linear interpolation) vs. point-source, extended-source (quadratic interpolation) vs. point-source, extended-source comparison (quadratic vs. linear interpolation), extended-source comparison (cubic vs. quadratic), relative pixel position vs. wavelength.

2. Observations

The observations used in this analysis were obtained under proposal 8844, “Deep Spatial/Spectral PSF Calibration of STIS,” Charles Proffitt, principle investigator. We have used the subset of unocculted, $52 \times 0.2''$ long-slit medium resolution mode observations of the following stars: HD 181204 (M0, variable-irregular), HD 115617 (G5 V), HD 141653 (A2 IV), BD+75D325 (O5pvar).

3. The Pixel-Crossing Problem

As a spectral image is converted to an extended source image, the interpolation introduces artifacts in the data. These artifacts are apparent at the $\pm 3\%$ level in spectral extractions that use extraction heights less than the number of pixel crossings.

Figure 1 shows comparisons of 3-pixel extractions from spectral images rectified using three different interpolation methods (linear, quadratic, and cubic) against a standard point-source extraction (no interpolation, extraction height = 7 pixels). The observed (unrectified) spectrum of HD 181204 (observation ID O68M03090) crosses 7.5 CCD rows. Note that the cubic and quadratic methods yield the same results at the $\pm 1\%$ level. The relative pixel-crossing positions are shown at the bottom. The cycles in that plot are clearly correlated with the variations in the ratio plots. The spectrum was sub-sampled by a factor of four in the cross-dispersion direction and by two in the dispersion direction. The grating used was G750M.

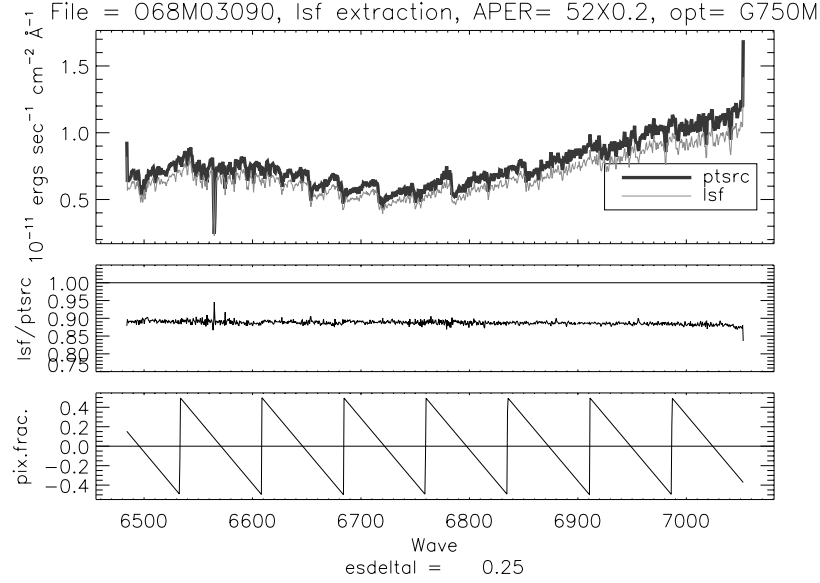


Figure 2. Optimal extraction of observation O68M03090 using the cross-dispersion profile array from observation O68M02080.

4. Optimal Extraction Using the Cross-Dispersion Profile

4.1. Long-Slit Cross-Dispersion Profile Derivation

A cross-dispersion profile may be derived as a function of pixel-crossing position from a rectified, background-subtracted observation. The columns for a particular pixel-crossing cycle (see bottom plot in Figure 1) are extracted from a rectified spectrum. The signal to noise for each column in the cycle is increased by averaging it together with its two neighboring columns. For each end column, the average is performed with its neighboring inside column. A record of the relative pixel-crossing position for each column is made. If the cross-dispersion profile array contains artifacts, it is rejected and the procedure is repeated for a different pixel-crossing cycle.

4.2. Optimal Extraction Method

The optimal extraction is performed column-by-column across the background-subtracted rectified spectral image. Each column in the observation is matched to a column in the cross-dispersion profile array by its pixel crossing value. Next, the relative offset between the profile and the data in the cross dispersion is determined (at this point manually). The optimal extraction algorithm described by Horne (1986) uses a linear regression method. The generalization of the single-source extraction to multiple-source extraction is made using the multiple linear regression method described by Bevington and Robinson (1992).

$$y(x_i) = \sum_{m=1}^k (a_k \times f_k(x_i)) \quad (1)$$

where x_i is a column element, $y(x_i)$ is the fitted function at x_i , m is the number of spectra to fit, f_k is the cross-dispersion profile co-aligned with the k th spectrum, a_k is the parameter of the fit, or the optimal extraction for the k th spectrum is the row of a_k in each column (wavelength).

The row matrix \underline{a} may be determined as follows: $\underline{a} = \underline{\beta} \times \underline{\alpha}^{-1}$, where $\beta_k \equiv \sum_i [\sigma_i^{-2} \times y_i \times f_k(x_i)]$ and $\alpha_{lk} \equiv \sum_i [\sigma_i^{-2} \times f_l(x_i) \times f_k(x_i)]$

5. Optimal Extraction: Single Point-Source Results

Figure 2 shows the optimal extraction result for observation O6M03090 (HD 181204) using a cross dispersion profile derived from observation O6M02080 (HD 115617). The top plot shows both the standard 7-pixel point-source extraction from the unrectified spectrum and the optimal extraction from the rectified (cubic interpolation) spectrum. The middle plot shows the ratio of the two extractions, and the bottom plot shows the relative row-pixel position. The cross-dispersion profile was created from the pixel-crossing cycle in the O6M02080 data between 6600 Å and 6700 Å. The overall residuals are very low ($< 2\%$) with a $\sim 5\%$ residual at the position of H α 6563 Å absorption. Correcting for the 10% offset seen in the (middle) ratio plot would require deriving a sensitivity curve using the optimal extraction method. Using the cross-dispersion profile array from O6M02080 to perform an optimal extraction on the O6M02080 spectrum itself (not shown) also produces small residuals (except at H α) but with a slight ($\sim 2\%$) drop from the blue end to the red end of the spectrum.

Deriving a profile array from O6M03090 for optimal extraction is not as successful, perhaps due to absorption features in the pixel crossing cycle between 6600 Å and 6700 Å, although no obvious artifacts are present in the profile array. When applying this array to the O6M03090 data itself, 2% column-to-column residuals are produced, and a overall 4% variation is observed from the blue to the red. Applying this profile array to O6M02080 produces 5% features in the residuals plot that correspond to the absorption features in O6M03090 between 6600 Å and 6700 Å. Also a 5% drop from the blue end of the spectrum to the red end is observed in the residuals.

6. Application to Simulated Point-Source Data

6.1. Creating the Simulated Blended Point-Source Spectra

Two test data-sets were created to monitor the effectiveness of point-source de-blending. Both used the standard star spectrum from observation O6M03090. In each case the rectified, background-subtracted spectrum was shifted, scaled and added to itself to produce an artificial spectral image with two spectra. The fits to the test data sets were made using the second complete pixel-crossing cycle from the short wavelength end of observation O6M02080. The first test set used an offset of 5 pixels and a scale factor of 5. The second test set used an offset of 25 pixels and a scale factor of 7.

6.2. Simulated Data: Extraction/Deblending Results

The extractions for both components of test data set 1 (5-pixel offset, scale factor=5) show large column-to-column residuals ($\sim 5\%$) and much larger variations ($\sim 20\%$) from the blue end of the spectrum to the red end when compared to the standard 7-pixel point-source extraction. The ratio plot of one component to the other has an average value of 2 with 20% variations. The average value should be 5, the input value of the scale factor for this test data set.

The extractions for both components of test data set 2 (25-pixel offset, scale factor = 7) also show large column-to-column residuals ($\sim 3\%$), but smaller variations across the whole spectrum. When compared to the standard point-source extraction, the residuals for the unscaled, unshifted component drop by 5% across the spectrum and show 2% features that are correlated with the relative pixel-crossing position. The scaled and shifted component residuals compared to the point source extraction is flat within the column-to-column 2% noise except for a 2% discontinuity coincident with the pixel-crossing cycle that begins on the blue side at ~ 6600 Å, and a 2% variation coincident with the pixel crossing cycle at the red end of the spectrum (> 6900 Å).

7. Conclusions/Directions

For isolated spectra, results comparable to the standard point-source extraction can be obtained using an optimal extraction method that relies upon the actual cross-dispersion profile instead of an analytic function. De-blending multiple spectra will clearly involve more work, particularly for very closely blended sources. More work remains to be done in verifying how robust the method is for handling isolated spectra, and in understanding how features in the spectrum, such as absorption and emission lines, affect the line-spread-function template. Future work will also include multiple source extractions of real data.

References

- Bevington, P. R. and Robinson, D. K., 1992, "Data Reduction and Error Analysis for the Physical Sciences," (New York: McGraw-Hill)
- Horne, K., 1986, PASP 98, 609